Shape Optimal Design Using Fictitious Loads

S. D. Rajan*
Arizona State University, Tempe, Arizona
and
A. D. Belegundu†
Pennsylvania State University, University Park, Pennsylvania

Implementation aspects of the natural velocity field approach for shape optimal design are discussed. The problem of concern is to find the optimum shape of an elastic body that requires minimizing an objective function subject to stress, displacement, frequency, and manufacturing constraints. In this paper, fictitious loads are applied at certain control nodes on an auxiliary structure, and the deformation produced by these loads is used to update the shape. The use of beam stiffeners in the auxiliary structure leads to smoother shapes. Furthermore, softer material properties in the auxiliary structure result in faster convergence when iterating through the feasibile region. The method is applied in conjunction with both discrete and continuum methods of design sensitivity analysis.

Introduction

In recent years, considerable interest has been shown in the development and use of shape optimal design codes. The reader is referred to the proceedings of two international conferences[1,2] and survey papers[3,4] for recent publications in this area. Recently, a method[5] based on fictitious loads acting on an auxiliary structure as design variables, using the associated displacements for internal node movement, was developed. That is, a natural velocity field is used to relate design variables and grid points. The reader is referred to Refs. 6 and 7 for an alternate formulation of natural velocity fields. Special attention is given to the problem of obtaining smooth optimum shapes. The role of the velocity field matrix, design sensitivity analysis, and smoothness of boundary as discussed herein also apply to shape design approaches based on geometric entities (such as spline or polynomial coefficients) chosen as design variables. It should be noted that a one-to-one correspondence exists between the fictitious loads used here and control point coordinates, as shown in Ref. 8. Thus, the use of a natural velocity field can be integrated with geometric design variables such as keypoint coordinates or spline coefficients.

Let $\boldsymbol{b}$ be a $(k \times 1)$ design variable vector and the domain Ω be parameterized as $\Omega = \Omega(\boldsymbol{b})$. Let $\Gamma(\boldsymbol{b})$ represent the changing boundary. Then, the problem of concern is to minimize

$$f(\boldsymbol{b}) \tag{1}$$

subject to

$$g(\boldsymbol{b}) = \sigma_{vm}/\sigma_a - 1 \le 0 \tag{2}$$

$$\boldsymbol{b}^L \le \boldsymbol{b} \le \boldsymbol{b}^U \tag{3}$$

$$\Gamma(\boldsymbol{b}) \epsilon V \tag{4}$$

where f = weight of the structure, σ_{vm} = von Mises stress, σ_a = allowable stress, $\boldsymbol{b}^L$ and $\boldsymbol{b}^U$ are lower and upper bounds, respectively, and V is a space or collection of functions that are sufficiently smooth and that satisfy design needs. The implementation discussed here can also be made to handle other types of costs and constraint functions because these are defined through user-supplied subroutines. The shape restriction in Eq. (4) is an important part of the problem definition; for example, parts of the boundary should be unchanged, straight edges should remain straight, etc. Furthermore, optimum shapes in the absence of this constraint may be very discontinuous and useless for engineering design.[3] This difficulty is addressed in the section on "Example Problems" later in this paper.

The role of the velocity field matrix and implementation of design sensitivity is discussed next. Emphasis is placed on generality, so that the rewriting of computer codes is kept to a minimum when mesh generators or user-defined requirements change. Attention is given to the case in which traction loads act on a changing boundary. Example problems using constant strain triangle, four-node quadrilateral, and eight-node solid isoparametric finite elements are presented.

Internal Node Movement: Velocity Field Matrix $[Q]$

Consider a finite-element model of a structure. There may be hundreds of grid points in the model. Consequently, a relatively small set of design variables must be chosen which characterizes the shape of the structure, and then the changes in these design variables must be related to changes in the grid point locations. This relation between design variables and internal node movements can be expressed by introducing a velocity field matrix $[Q]$ as follows. Let $\boldsymbol{G}$ be an $(n \times 1)$ vector of grid point locations consisting of the X, Y, and Z coordinates of each node. Then, define the relation

$$\delta \boldsymbol{G} = [Q]\delta \boldsymbol{b} \tag{5}$$

where $[Q] = [\mathrm{d}\boldsymbol{G}/\mathrm{d}\boldsymbol{b}]$ is the velocity field matrix of dimension $(n \times k)$. The $[Q]$ matrix is generated (once every few iterations) herein using natural entities: specifically, using displacements produced by fictitious loads acting on an auxiliary structure. Thus, the velocity field matrix is generated using

$$[K_a]\boldsymbol{q}^i = \boldsymbol{l}^i \tag{6}$$

Received Aug. 24, 1987; revision received April 8, 1988; presented as Paper 88-2300 at the 29th AIAA/ASCE/ASME/AHS Structures, Structural Dynamics and Materials Conference, Williamsburg, VA, April 18–20, 1988.

*Assistant Professor, Civil Engineering Department.
†Assistant Professor, Mechanical Engineering Department.

where $[K_a]$ is the stiffness matrix of the auxiliary structure, q^i the ith column of $[Q]$, and l^i a load vector with only a unit load acting along i.

Note that geometric mesh generators can also be used to generate $[Q]$.[9-13] Care should be taken, however, in generating the velocity field matrix $[Q]$. Manufacturing requirements, such as a straight edge remaining straight or portions of the boundary remaining unchanged, should be satisfied. Furthermore, kinks in the boundary surface should be avoided. This kinking can happen when mapped mesh generators are used which operate on one segment or patch (created usually by a cell decomposition solid modeler) of the boundary at a time without maintaining shape continuity across patches. User-defined requirements that the shape should satisfy dictate the choice of design variables. In this paper, the user has the flexibility to model the auxiliary structure so that the displacements q^i obtained from Eq. (6) satisfy the designer's needs.

Design Sensitivity Analysis

Shape optimization methods can be implemented using either discrete or continuum methods of design sensitivity analysis. Both the semianalytical method and the domain method have been implemented herein.

Semianalytical Method

Consider an implicit "active" constraint function $g_i(b,z)$, where the displacement vector z is obtained from the finite-element equations $[K(b)]z = F(b)$, with K the structural stiffness matrix and F a nodal load vector. In the discrete adjoint method, the gradient of g_i is given by

$$\frac{dg_i}{db} = \frac{\partial g_i}{\partial b} - \lambda^T \frac{\partial}{\partial b}[K(b)z - F(b)] \tag{7}$$

where the adjoint vector λ is obtained by solving

$$[K]\lambda = \frac{\partial g_i^T}{\partial z} \tag{8}$$

The derivative of the stiffness matrix, $\partial K/\partial b_i$, $i = 1,\ldots,k$, is computed here using a divided difference formula as follows. In view of Eq. (5), the grid point vector as a result of a perturbation in the jth variable is $G^\epsilon = G^0 + \epsilon q^j$, where G^0 represents the current shape. The approximate derivative is then given by

$$\frac{\partial K}{\partial b_j} = \frac{[K(G^\epsilon) - K(G^0)]}{\epsilon} \tag{9}$$

Although the approximate derivative based on Eq. (9) requires reassembly of the stiffness matrix k times, it offers a simple approach for implementing shape sensitivity into commercial finite-element programs having a large element library. Furthermore, this assembly is preferably done element-wise. The method has proved to be accurate enough for the isoparametric elements used in this paper. Note that the preceding sensitivity expressions can be coded for any $[Q]$. That is, the Q-matrix generation is independent of the constraint sensitivity calculations and should be coded separately. The implication is that changing the mesh generator or switching from a natural to a geometric $[Q]$ will not require changes in the entire program.

In problems in which normal traction loads are acting on the boundary (such as hydrostatic pressure), the sensitivity analysis should include the contribution from the changing load as the shape is changed. Thus, if the traction force on an element is given by

$$T^e = T_0 n \tag{10}$$

where T_0 is its (constant) magnitude and $n = n(b)$ is the unit normal to the boundary which depends on the boundary shape, then the sensitivity expression is

$$\frac{dT^e}{db} = T_0 \frac{dn}{db} \tag{11}$$

Note that the load vector F is a function of the design variables. Because the nodal load vector F in the finite-element equation $[K]z = F$ is assembled from the element traction forces, the derivative dF/db is readily obtained using Eq. (11) and can then be substituted into Eq. (7).

Domain Method

In the domain method,[5,14,15] the change in shape is thought of as a deformation of a continuum. Details are not presented here, but emphasis is placed on a general implementation of the method. Specifically, consider the weight of a thin plate:

$$F = \int_\Omega \rho g \, d\Omega \tag{12}$$

where Ω is the domain of the plate. Then the sensitivity expression is

$$\frac{df}{db} = \sum \left[t_e \int \rho g \nabla \cdot N \, dA \right] [Q^e] \tag{13}$$

where t_e is the element thickness, ρ = density, g = acceleration due to gravity, N = finite-element shape functions, and ∇ = differential operator, and where $[Q^e]$ is obtained by selecting appropriate elements from the velocity field matrix $[Q]$. The calculation of df/db is done element-wise and is similar to the assembly of the load vector from element load vectors in the finite-element method. The sensitivity expression for stress constraints takes the form

$$\frac{dg_i}{db} = \sum \left[t_e \int \psi \, dA \right] [Q^e] \tag{14}$$

where ψ is a known function depending on N and its derivatives, and g_i is the ith active constraint. Here, the emphasis is on the fact that the Q matrix should be generated separately and simply enters as a product in the sensitivity expressions in Eqs. (13) and (14). Thus, the domain method can be integrated with any type of mesh generator or natural approach which generates $[Q]$.

The problem of normal traction forces on a changing two-dimensional boundary involves determination of the material derivative of a line integral of the form[5]

$$I = \int_{1\text{-}2} p^T T \, d\Gamma \tag{15}$$

where 1-2 represents the boundary or edge of an element connecting nodes 1 and 2, p is an adjoint function, and T is the traction. The basic concept here is to use the isoparametric concept and transform the preceding integral to one with fixed limits of integration, as

$$I = \int_0^1 p(\xi) T(\xi) \ell_{1\text{-}2} \, d\xi \tag{16}$$

The material derivative of the preceding integral can now be obtained readily. Again, this derivative will involve rows of $[Q]$.

Example Problems

Four problems are solved here using the DIHARD and OPTECH systems.[16] The material properties used are those for steel. The following symbolic notation is used: E = Young's modulus, ρ = mass (or weight) density, ν = Poisson's ratio, NE = number of elements, and NN = number of nodes.

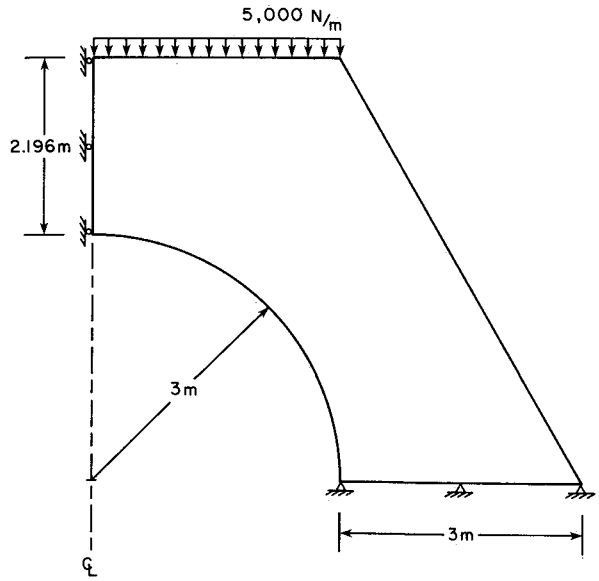

Fig. 1 Culvert problem.

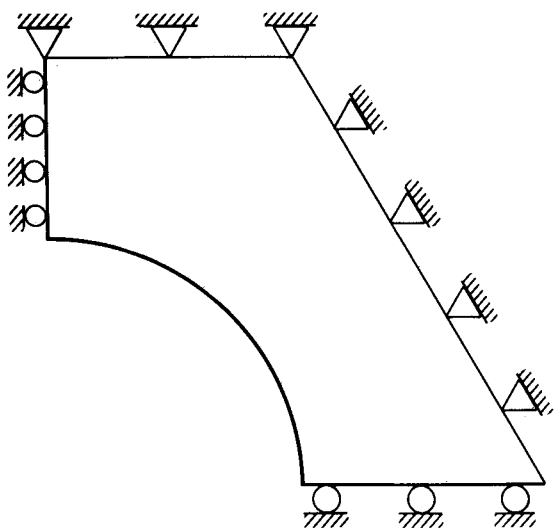

Fig. 2 Auxiliary structure.

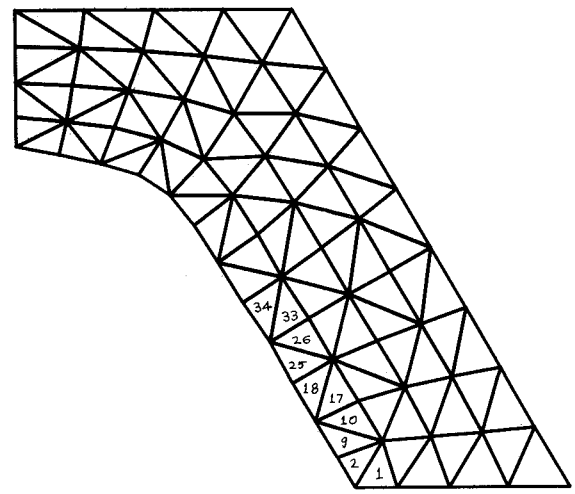

Fig. 3 Optimum shape with CST elements.

Table 1 Stress distribution along hole with CST elements

Element	1	2	9	10	17	18	25	26	33	34
σ_{vm}/σ_a	0.67	1.0	0.95	0.74	0.73	0.94	0.96	0.75	0.76	0.97

Culvert

Results using both constant strain triangle (CST) and four-node quadrilateral (QM4) elements are given for the culvert problem (Fig. 1). The objective is to minimize the weight (or area) by changing the shape of the inner hole while keeping the outer boundary fixed. This is a plane strain problem, and, owing to symmetry, only one-half of the structure is considered. The von Mises stress constraint is imposed within each finite element. The boundary conditions for the primary (original) and auxiliary structures are shown in Figs. 1 and 2, respectively.

Twenty-four fictitious loads, which are the design variables, are applied along the hole; $E = 20 \times 10^6$ psi, $\nu = 0.3$, $\rho = 0.743$ E-3 lbm/in.^{3}, $\sigma_a = 15{,}000$ psi, $NE = 77$, and $NN = 96$. Note that the boundary conditions for the auxiliary structure satisfy the user requirement that the outer boundary remain unchanged. With CST elements, the initial design corresponds to an 11% violation in the stress constraint. The optimum shape (Fig. 3) corresponds to a 13% reduction in weight, from 11.98×10^{-3} lbm to 10.39×10^{-3} lbm. Furthermore, the shape is smooth. The optimum shape shown in Fig. 3 required 12 iterations.

Interestingly, continuation of the iterative process leads to the generation of a sawtooth shape; see the shapes after 15 and 26 iterations, respectively, in Fig. 4. Although the weight reduction after 26 iterations is 19%, the final shape is not a solution because the smoothness requirement is part of the problem statement [see Eq. (4)]. This sawtooth shape, which is obviously unacceptable, can be explained by examining the stress distribution along the hole at the end of the twelfth iteration. Referring to Fig. 3 and Table 1, we see that triangular elements that have two nodes on the boundary have much higher stress compared to those that have only one. Thus, a high-low type of varying stress pattern is predicted by the model. Evidently, element stress averaging will alleviate this problem and lead to smoother and better solutions. This point has also been noted in Ref. 9. Although element stress smoothing is a well-known concept in finite-element literature,[17] its use in shape optimal design also is important. Of course, adaptive modeling,[11] whereby larger number of elements are introduced into the model, is necessary after every few iterations when elements become highly distorted and stress gradients across elements are high. But even here, stress smoothing is advantageous.

The culvert problem is also solved using four-node quadrilateral (QM4) elements with Gauss quadrature integration. The initial design is feasible, and the final shape (Fig. 5) corresponds to a 19% reduction in weight. Whereas the greater reduction can be attributed, at least in part, to the fact that the QM4 element is less stiff than the CST element and predicts smaller stresses, the QM4 elements also lead to a smoother optimum shape. This is because, referring to Fig. 5 and Table 2, the stress distribution along the hole is more uniform compared to the CST model. The general superiority of the QM4 element over CST elements, for shape problems such as this where maximum stress occurs along a boundary, is thus established.

Finally, the culvert problem has also been solved using CST elements and pressure loads as design variables.[5] Five design variables are used, corresponding to the magnitudes of five pressure distributions along the hole. Pressure loading results in a reduction in the number of design variables through a natural linking. The optimum shape corresponds to a 13% reduction and is shown in Fig. 6.

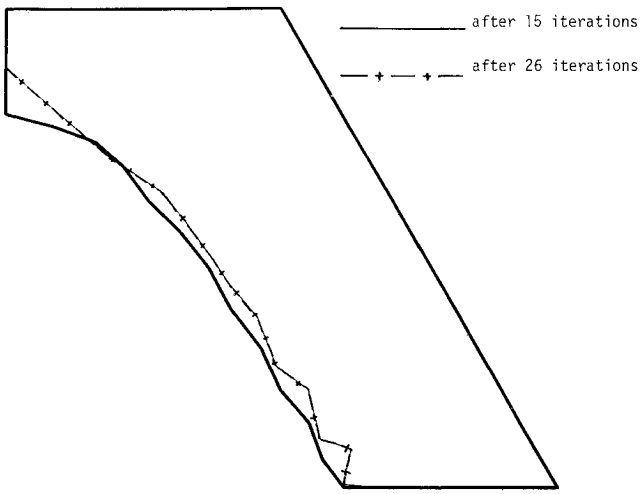

Fig. 4 Generation of sawtooth pattern.

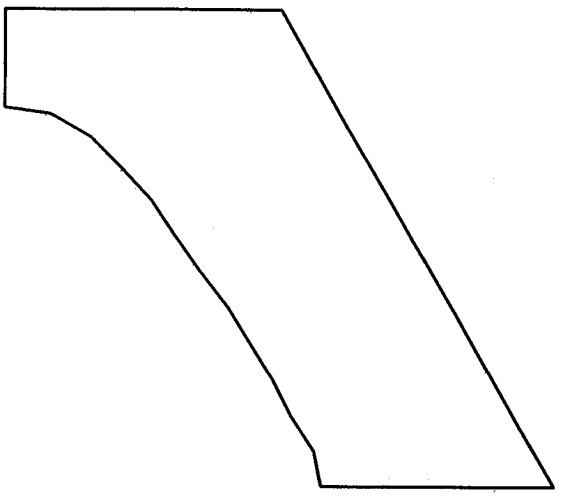

Fig. 6 Optimum shape using pressure loads as design variables.

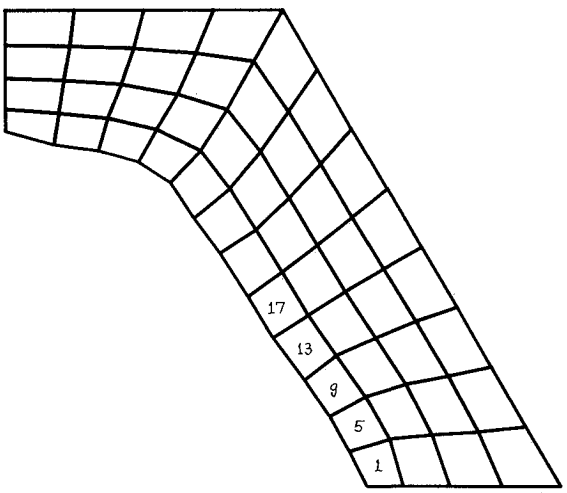

Fig. 5 Optimum shape with QM4 elements.

Table 2 Stress distribution along hole with QM4 elements

Element	1	5	9	13	17
σ_{vm}/σ_a	0.90	0.94	0.97	0.95	0.94

Fillet

Consider the fillet shown in Fig. 7. The problem is to determine the optimum shape of the edge 4–5 while keeping the rest of the boundary fixed. The thickness is optimized first using fully stressed design.[16] The primary and auxiliary structures are modeled with CST elements. In addition, beam stiffeners are used along edge 4–5 in the auxiliary structure to obtain a smooth shape; $E = 20 \times 10^6$ psi, $\nu = 0.3$, $w = 120$ ksi (normal to edge 1–5), $\sigma_a = 120$ ksi, $NE = 349$, and $NN = 231$. The number of design variables is eight, consisting of pressure loads. The final shape obtained after nine iterations is shown in Fig. 8. The initial and final areas are 155.25 and 139.80 in.^{2}, yielding a 10% reduction. As with other examples, the method is seen to produce relatively low element distortions in the finite-element mesh corresponding to the optimized structure.

Torque Arm

A torque arm[4] is shown in Fig. 9. The primary structure is modeled using CST elements. In the auxiliary structure, beam stiffeners are used all along the outer boundary and along the slot boundary. Furthermore, two beam elements are used across the slot, at the right end, to prevent the slot from closing and creating a sharp corner. The shape and location of the (circular) holes are fixed; $E = 30 \times 10^6$ psi, $\nu = 0.3$, $\rho = 0.734$ E-3 lbm/in.^{3}, $\sigma_a = 15{,}000$ psi, $NE = 196$, and $NN = 148$. The thickness has been optimized. The number of design variables is 18 (pressure loads). The final shape is shown in Fig. 10. The initial mass is 0.2234 lbm, and the final mass is 0.1548 lbm, yielding a 31% reduction, obtained in 15 iterations.

Three-Dimensional Cantilever Beam

The problem of maintaining a smooth boundary is well exemplified by the three-dimensional cantilever beam problem first examined by Imam.[18] Unless special care is given to boundary smoothness, the optimum shape is very irregular and unacceptable. Here, beam stiffeners are used to generate a smooth shape. Consider the $3 \times 3 \times 18$-in. beam in Fig. 11 drawn in perspective view, fixed at one end and loaded at the other. The total load at the free end = 2000 lb. The beam is modeled using eight-node solid (SLD8) elements; $E = 29.5 \times 10^6$ psi, $\nu = 0.29$, $\sigma_a = 15{,}000$ psi, $NE = 64$, and $NN = 135$. The initial design is feasible.

The auxiliary structure is also modeled using SLD8 elements, and fictitious pressure loads are applied at the free end of the beam (Fig. 12), with a total of two design variables. In addition, the auxiliary structure is modeled using longitudinal beam elements (Fig. 13) along the boundary. Because beam deflections are Hermite cubics, the optimized shape can be expected to be smooth. This is, in fact, the case, as shown in Fig. 14, corresponding to a 32% reduction in weight. The effect of the beam stiffeners is to insure that the velocity field obtained from Eq. (6) is acceptably smooth.

In the beam problem discussed earlier, the initial design is feasible. Thus, there is no need to let the support nodes move, and the primary and auxiliary structures have the same boundary conditions. For initially infeasible designs, however, the auxiliary structure should be modeled so as to allow the support nodes to move in the plane of the cross section. The solution of this problem requires the following more general velocity field:

$$[Q] = [Q^1 Q^2]$$

where $[Q^1]$ and $[Q^2]$ are obtained by solving Eq. (6) with two different auxiliary structures having different boundary conditions.

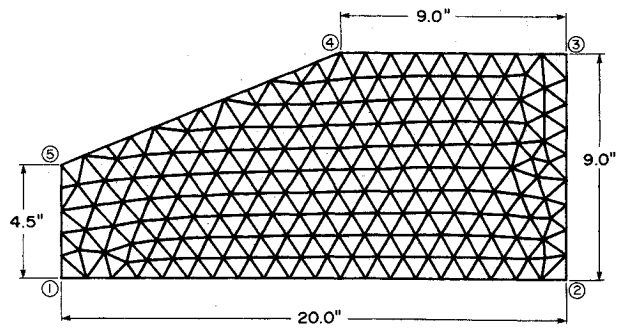

Fig. 7 Fillet problem.

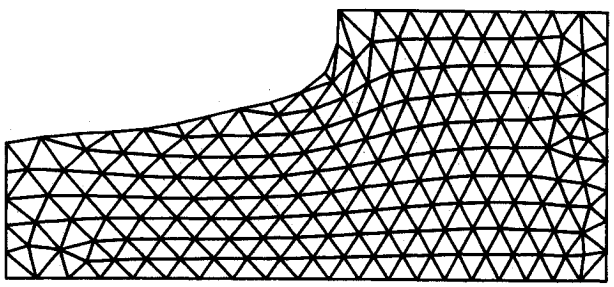

Fig. 8 Optimized fillet.

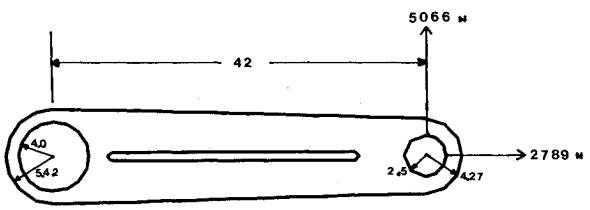

Fig. 9 Torque arm problem.

Fig. 10 Optimized torque arm.

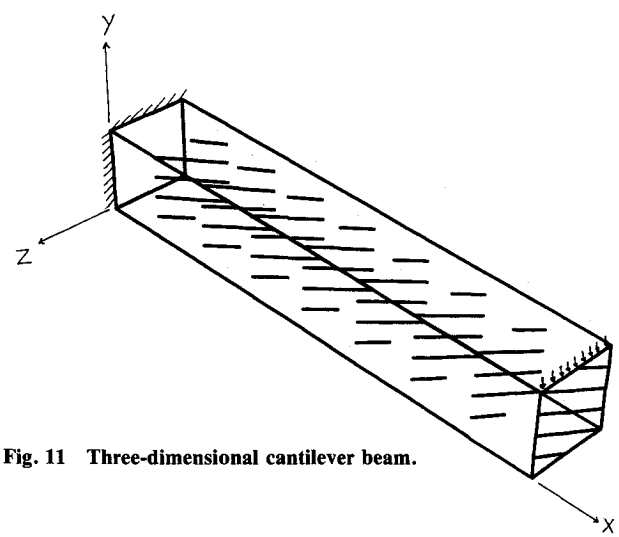

Fig. 11 Three-dimensional cantilever beam.

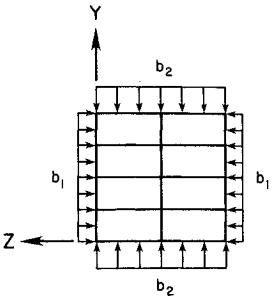

Fig. 12 Design variables.

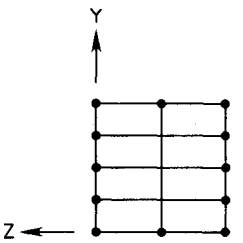

Fig. 13 Longitudinal beam stiffeners in auxiliary structure.

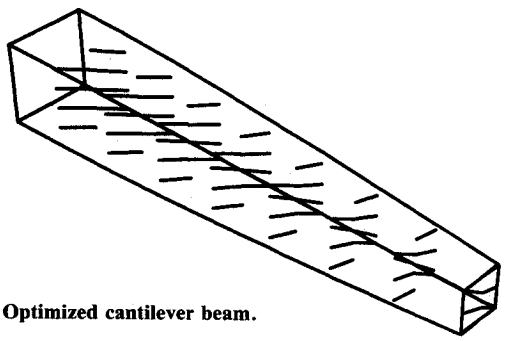

Fig. 14 Optimized cantilever beam.

Conclusions

A general implementation of shape optimal design methods using the natural velocity field approach has been discussed. The main points are as follows. The generation of the velocity field matrix $[Q]$ should be coded separately from subsequent design sensitivity calculations. For the isoparametric finite elements considered here, the semianalytical method of design sensitivity is simple to implement for a library of elements. The domain method is computationally less expensive, however. The special treatment of traction loads acting on a changing boundary is dealt with in both semianalytical and domain-sensitivity approaches.

The use of element stress smoothing[9] is motivated from the study of the culvert problem. Smoother and more optimal shapes can be expected to result. Furthermore, the quadrilateral element is shown to be superior to the CST element for problems in which maximum stress occurs on the boundary. The use of beam stiffeners for the auxiliary structure leads to a dramatic difference in the smoothness of the optimized shape. From a physical viewpoint, this is to be expected. It is observed from the example problems that the use of a natural velocity field produces meshes with relatively low element distortions. Similar observations have been made in Refs. 6 and 7.

Acknowledgments

This research is supported by NSF Grants DMC 86-14205 and DMC 86-13438. The authors thank Dr. Wayne Nack and Professor T. R. Chandrupatla for giving valuable ideas on this topic.

References

[1]Bennett, J. A. and Botkin, M. E., (eds.), "The Optimum Shape: Automated Structural Design," International Symposium sponsored by General Motors Research Labs., Plenum, New York, 1985.

[2]Dulikravich, G., (ed.), *Proceedings of the 2nd International Conference on Inverse Design Concepts and Optimization in Engineering Sciences, ICIDES-II,* the Pennsylvania State Univ., University Park, PA, Oct. 1987.

[3]Haftka, R. T. and Grandhi, R. V., "Structural Shape Optimization—A Survey," *Computer Methods in Applied Mechanics and Engineering,* Vol. 57, 1986, pp. 91–106.

[4]Ding, Y., "Shape Optimization of Structures: A Literature Survey," *Computers and Structures,* Vol. 24, No. 6, 1986, pp. 985–1004.

[5]Belegundu, A. D. and Rajan, S. D., "A Shape Optimization Approach Based on Natural Design Variables and Shape Functions," *Computer Methods in Applied Mechanics and Engineering,* Vol. 66, 1988, pp. 87–106.

[6]Choi, K. K. and Yao, T. M., "3-D Modeling and Automatic Regridding in Shape Design Sensitivity Analysis," *Proceedings of the Symposium on Sensitivity Analysis in Engineering,* NASA Langley Research Center, Hampton, VA, NASA CP 2457, Sept. 1986, pp. 329–346.

[7]Choi, K. K., "Shape Design Sensitivity Analysis and Optimal Design of Structural Systems," *Computer Aided Optimal Design,* edited by C. A. Mota Soares, Springer-Verlag, Heidelberg, 1987, pp. 439–492.

[8]Rajan, S. D. and Belegundu, A. D., "A Shape Optimization Approach Using Fictitious Loads as Design Variables," AIAA Paper 87-0834, April 1987.

[9]Yang, R. J. and Botkin, M. E., "A Modular Approach for Three-Dimensional Shape Optimization of Structures," AIAA Paper 86-1009, May 1986.

[10]Braibant, V., Fleury, C., and Beckers, P., "Shape Optimal Design: An Approach Matching CAD and Optimization Concepts," Aerospace Lab., Univ. of Liège, Belgium, Rept. SA-109, 1983.

[11]Botkin, M. E. and Bennett, J. A., "Shape Optimization of Three-Dimensional Folded Plate Structures," *AIAA Journal,* Vol. 23, Nov. 1985, pp. 1804–1810.

[12]Queau, J. P. and Trompette, P., "Optimum Shape Design of Turbine Blades," *Transactions of the ASME,* Vol. 105, Oct. 1983, pp. 444–448.

[13]Wasserman, K., "Three-Dimensional Shape Optimization of Arch Dams with Prescribed Shape Functions," *Journal of Structural Mechanics,* Vol. 11, No. 4, 1983–84, pp. 465–489.

[14]Choi, K. K. and Seong, H. G., "A Domain Method for Shape Sensitivity Analysis of Built-Up Structures," *Journal for Computer Methods in Applied Mechanics and Engineering,* Vol. 57, 1986, pp. 1–15.

[15]Hou, J. W., Chen, J. L., and Sheen, J. S., "Computational Method for Optimization of Structural Shapes," *AIAA Journal,* Vol. 24, June 1986, pp. 1005–1012.

[16]Rajan, S. D. and Budiman, J., "Study of Two-Dimensional Plane Elasticity Finite Elements for Optimal Design," *Journal of Mechanics of Structures and Machines,* Vol. 15, No. 2, 1987, pp. 185–207.

[17]Zienkiewicz, O. C., *The Finite Method,* 3rd ed., McGraw-Hill, New York, 1979.

[18]Imam, M. H., "Three-Dimensional Shape Optimization," *International Journal for Numerical Methods in Engineering,* Vol. 18, 1982, pp. 661–673.